Preparation and Characterization of (Tetrabenzoporphyrinato)cobalt(II) Iodide, a Ring-Oxidized Molecular Conductor

Kwangkyoung Liou,[†] Timothy P. Newcomb,[†] Michael D. Heagy,[‡] Julia A. Thompson,[†] William B. Heuer,[‡] Ronald L. Musselman,[‡] Claus S. Jacobsen,[§] Brian M. Hoffman,*[,†] and James A. Ibers*[,†]

Department of Chemistry and Materials Research Center, Northwestern University, Evanston, Illinois 60208-3113, Department of Chemistry, Franklin and Marshall College, Lancaster, Pennsylvania 17604, and Physics Laboratory III, Technical University of Denmark, DK-2800 Lyngby, Denmark

Received January 7, 1992

Oxidation of (tetrabenzoporphyrinato)cobalt(II), Co(tbp), with iodine affords Co(tbp)I. The structure comprises metal-over-metal columnar stacks of partially (one-third) oxidized Co(tbp) groups surrounded by chains of I_3^- ions. Co(tbp)I crystallizes in the tetragonal space group $D_{4h}^2 - P4/mcc$ with $a = 14.129$ (3) Å, $c = 6.334$ (1) Å, $V = 1249$ Å^3, and $Z = 2$. In contrast to (phthalocyaninato)cobalt(II) iodide, Co(pc)I, which shows metal oxidation and is a metal-spine conductor, conductivity and thermoelectric power measurements on Co(tbp)I show that oxidation occurs at the macrocycle; the charge carriers are holes in the five-sixths-filled band comprising overlapping p–π orbitals from adjacent tbp rings. Reflectance spectroscopy measurements on single crystals provide an explanation of why the tbp macrocycle is more readily oxidized: the p–π orbitals are higher in energy for Co(tbp)I than for Co(pc)I. Ring oxidation of Co(tbp) leaves one spin on each Co^{2+} ion. However, Co(tbp)I does not exhibit an EPR signal associated with either the carriers or the Co^{2+} ($S = {}^1/_2$) ions, and the magnetic susceptibility data yield a Curie constant of 0.039 (emu K)/mol, far less than expected for a linear chain of $S = {}^1/_2$ spins. In addition, Co(tbp)I does not have a measurable magnetoconductance, as would be expected from a system with conduction electrons scattered by reorientable local moments. This is in contrast to Cu(pc)I, which also is ring oxidized with the metal ion and carriers forming a spin-coupled system, but which shows both the full Curie constant ($C = 0.4$ (emu K)/mol) for the Cu^{2+} ($S = {}^1/_2$) ions and an EPR signal. Thus, spins in the $Co^{2+}(d_{z^2})$ orbitals of a partially oxidized Co(tbp) stack must exhibit antiferromagnetic coupling through direct or carrier-mediated interactions, or most likely both, that is much stronger than in Cu(pc)I.

Introduction

Molecular conductors may be divided into two classes: organic molecular metals that conduct through overlapping p–π orbitals[1] and linear-chain metal-spine conductors that transport charge through metal-based d_{z^2} orbitals.[2] In the chemically versatile but structurally similar porphyrinic molecular conductors, M(L)-A_x, charge transport is introduced by partial oxidation of the M(L) moiety.[3-13] The site of oxidation, and thus of charge transport, can be changed by tuning the local electronic structure of M(L) through incorporation of different transition metals into the same macrocycle. For example, both Ni(pc)I and Cu(pc)I are (one-third) ring-oxidized conductors with charge transport through the highest-occupied delocalized π molecular orbitals of pc.[3,5] However, Co(pc)I is partially oxidized at the central metal with the result that conduction is through the overlapping d_{z^2} orbitals.[4] Thus, replacing Ni or Cu with Co in M(pc)I compounds changes the site of charge transport from ring-centered to metal-centered. Furthermore, in the series of "alloys" Co_xNi_{1-x}(pc)I

[†] Northwestern University.
[‡] Franklin and Marshall College.
[§] Technical University of Denmark.

(1) (a) *Proceedings of the International Conference on the Science and Technology of Synthetic Metals*; Hanack, M., Roth, S., Schier, H., Eds.; Elsevier Sequoia: Lausanne, Switzerland, 1991; Vols. 42 and 43. (b) Cowan, D. O.; Wiygul, F. M. *Chem. Eng. News* **1986**, *64* (29), 28–45.
(2) (a) Ferraro, J. R.; Williams, J. M. *Introduction to Synthetic Electrical Conductors*; Academic Press: New York, 1987; pp 139–204. (b) Williams, J. M.; Schultz, A. J.; Underhill, A. E.; Carneiro, K. In *Extended Linear Chain Compounds*; Miller, J. S., Ed.; Plenum Press: New York, 1982; Vol. 1, pp 73–118. (c) Miller, J. S.; Epstein, A. J. *Prog. Inorg. Chem.* **1976**, *20*, 1–151.
(3) (a) Schramm, C. J.; Scaringe, R. P.; Stojakovic, D. R.; Hoffman, B. M.; Ibers, J. A.; Marks, T. J. *J. Am. Chem. Soc.* **1980**, *102*, 6702–6713. (b) Martinsen, J.; Greene, R. L.; Palmer, S. M.; Hoffman, B. M. *J. Am. Chem. Soc.* **1983**, *105*, 677–678. (c) Martinsen, J.; Palmer, S. M.; Tanaka, J.; Greene, R. L.; Hoffman, B. M. *Phys. Rev. B* **1984**, *30*, 6269–6276. (d) Toscano, P. J.; Marks, T. J. *J. Am. Chem. Soc.* **1986**, *108*, 437–444.
(4) Martinsen, J.; Stanton, J. L.; Greene, R. L.; Tanaka, J.; Hoffman, B. M.; Ibers, J. A. *J. Am. Chem. Soc.* **1985**, *107*, 6915–6920.
(5) (a) Ogawa, M. Y.; Martinsen, J.; Palmer, S. M.; Stanton, J. L.; Tanaka, J.; Greene, R. L.; Hoffman, B. M.; Ibers, J. A. *J. Am. Chem. Soc.* **1987**, *109*, 1115–1121. (b) Ogawa, M. Y.; Hoffman, B. M.; Lee, S.; Yudkowsky, M.; Halperin, W. P. *Phys. Rev. Lett.* **1986**, *57*, 1177–1180.
(6) Martinsen, J.; Pace, L. J.; Phillips, T. E.; Hoffman, B. M.; Ibers, J. A. *J. Am. Chem. Soc.* **1982**, *104*, 83–91.
(7) (a) Liou, K. K.; Ogawa, M. Y.; Newcomb, T. P.; Quirion, G.; Lee, M.; Poirier, M.; Halperin, W. P.; Hoffman, B. M.; Ibers, J. A. *Inorg. Chem.* **1989**, *28*, 3889–3896. (b) Quirion, G.; Poirier, M.; Liou, K. K.; Ogawa, M. Y.; Hoffman, B. M.; Ibers, J. A. *Phys. Rev. B* **1988**, *37*, 4272–4275.
(8) Pace, L. J.; Martinsen, J.; Ulman, A.; Hoffman, B. M.; Ibers, J. A. *J. Am. Chem. Soc.* **1983**, *105*, 2612–2620.
(9) Liou, K. K.; Jacobsen, C. S.; Hoffman, B. M. *J. Am. Chem. Soc.* **1989**, *111*, 6616–6620.
(10) (a) Ogawa, M. Y.; Palmer, S. M.; Liou, K. K.; Quirion, G.; Thompson, J. A.; Poirier, M.; Hoffman, B. M. *Phys. Rev. B* **1989**, *39*, 10682–10692. (b) Quirion, G.; Poirier, M.; Liou, K. K.; Hoffman, B. M. *Phys. Rev. B* **1991**, *43*, 860–864.
(11) (a) Godfrey, M. R.; Newcomb, T. P.; Hoffman, B. M.; Ibers, J. A. *J. Am. Chem. Soc.* **1990**, *112*, 7260–7269. (b) Newcomb, T. P.; Godfrey, M. R.; Hoffman, B. M.; Ibers, J. A. *Inorg. Chem.* **1990**, *29*, 223–228. (c) Newcomb, T. P.; Godfrey, M. R.; Hoffman, B. M.; Ibers, J. A. *J. Am. Chem. Soc.* **1989**, *111*, 7078–7084.
(12) (a) Almeida, M.; Kanatzidis, M. G.; Tonge, L. M.; Marks, T. J.; Marcy, H. O.; McCarthy, W. J.; Kannewurf, C. R. *Solid State Commun.* **1987**, *63*, 457–461. (b) Inabe, T.; Marks, T. J.; Burton, R. L.; Lyding, J. W.; McCarthy, W. J.; Kannewurf, C. R.; Reisner, G. M.; Herbstein, F. H. *Solid State Commun.* **1985**, *54*, 501–503. (c) Inabe, T.; Marks, T. J.; Lyding, J. W.; Burton, R. L.; Kannewurf, C. R. *Mol. Cryst. Liq. Cryst.* **1985**, *118*, 353–356.
(13) (a) Yakushi, K.; Yamakado, H.; Ida, T.; Ugawa, A. *Solid State Commun.* **1991**, *78*, 919–923. (b) Yakushi, K.; Sakuda, M.; Hamada, I.; Kuroda, H.; Kawamoto, A.; Tanaka, J.; Sugano, T.; Kinoshita, M. *Synth. Met.* **1987**, *19*, 769–774. (c) Yakushi, K.; Ida, T.; Ugawa, A.; Yamakado, H.; Ishii, H.; Kuroda, H. *J. Phys. Chem.* **1991**, *95*, 7636–7641.

0020-1669/92/1331-4517$03.00/0

the site of oxidation shifts from the macrocycle to the metal as x increases.[9]

The local electronic structure of M(L) compounds also can be varied by employing different macrocycles, with porphyrins generally being easier to oxidize than phthalocyanines. Therefore, we sought to determine whether isostructural Co(L)I molecular conductors that employ two different macrocycles, but incorporate the same metal ion, might yet exhibit oxidation at different sites. Typically, oxidation of cobalt(II) porphyrins and phthalocyanines occurs at the cobalt site to afford $[Co^{3+}(L)]^+$;[14] thus, metal ion oxidation in Co(pc)I is not unexpected. However, Co(II) porphyrins, such as (octaethylporphyrinato)cobalt(II) (Co^{2+}(OEP)), apparently undergo a one-electron ring-centered oxidation to give $[Co^{2+}(OEP^{\cdot+})][ClO_4^-]$.[15] Accordingly, would the porphyrin structural analogue of Co(pc), namely Co(tbp), exhibit oxidation at the ring or metal ion when it is partially oxidized to a molecular conductor? We have prepared Co(tbp)I, and we find that unlike Co(pc)I it is oxidized at the ring by iodine to form a ring-centered conductor that may be described formally as $[Co^{2+}(tbp)]^{0.33+}I_3^-{}_{0.33}$. These electronic structural features that cause the differences between M(pc)I and M(tbp)I are probed here with detailed UV–vis reflectance spectroscopic measurements.

Experimental Section

Synthesis of Zn(tbp). Zinc acetate dihydrate was synthesized by the reaction of zinc shot (AESAR, 99.9999%) with freshly distilled acetic acid. Zn(tbp) was synthesized by the template cyclization of 2-acetylbenzoic acid with this zinc acetate dihydrate by the method of Vogler and Kunkely,[16] but with a different purification process. Zn(tbp) was extracted from the reaction mixture with pyridine and then recrystallized from 1-chloronaphthalene.

Synthesis of H_2(tbp). Metal-free tbp was obtained by the demetalation of Zn(tbp) in concentrated sulfuric acid. The sulfuric acid solution of Zn(tbp) was neutralized by filtering it into a mixture of NH_4OH and ice. The resulting precipitate was washed with boiling water and dried, before being extracted with 1-chloronaphthalene in a hot-extraction apparatus.[17] The resultant material, H_2(tbp), obtained after cooling has a blue-purple luster; its optical spectrum shows no trace of Zn(tbp). The H_2(tbp) is further purified by sublimation at 350 °C under vacuum (less than 10^{-3} Torr). Anal. Calcd for $C_{36}H_{22}N_4$: C, 84.68; H, 4.34; N, 10.97. Found: C, 84.31; H, 4.24; N, 11.01 (Micro-Tech Labs, Inc., Skokie, IL).

Synthesis of Co(tbp). Co(tbp) was prepared by reaction of H_2(tbp) with bis(acetylacetonato)cobalt(II) [Co(acac)$_2$] in refluxing 1-chloronaphthalene. To 100 mL of 1-chloronaphthalene were added 500 mg (0.98 mmol) of H_2(tbp) and a large excess (~10 mmol) of Co(acac)$_2$, and the mixture was refluxed overnight. After the solution was cooled, the solid material was collected by filtration, washed in boiling water and acetone to remove any unreacted metal salts, and then dried. The sublimation of this material resulted in blue-purple crystals of Co(tbp) (overall yields 70–95%).

Synthesis of Co(tbp)I. Solutions of Co(tbp) in either 1,2,4-trichlorobenzene or 1-chloronaphthalene were oxidized with a 20% excess of molecular iodine in an H-tube equipped with a pressure-equalizing bridge. After the metallomacrocycle side of the H-tube was heated to 180–200 °C for 1 day, shiny dark-green needles of Co(tbp)I were collected by filtration. Anal. Calcd for $C_{36}H_{20}CoIN_4$: C, 62.27; H, 2.90; N, 8.07; I, 18.27. Found: C, 62.27; H, 2.85; N, 7.94; I, 18.18.

Resonance Raman Spectroscopy. Raman spectra were obtained as described previously.[3,18]

Table I. Crystal Data and Experimental Details for Co(tbp)I

formula	$C_{36}H_{20}CoIN_4$
fw	694.4
space group	D_{4h}^2–$P4/mcc$
a, Å	14.129 (3)
c, Å	6.334 (1)
V, Å^3	1249
Z	2
temp, K	125
d_{calc}, g/cm^3	1.845 (125 K)
λ(Cu Kα_1) radiation, Å	1.540 56
μ, cm^{-1}	157.3
transm factors	0.39–0.67
$R(F_o^2)^a$	0.085
$R_w(F_o^2)^a$	0.120
$R(F_o)^a$ for $F_o^2 > 3\sigma(F_o^2)$	0.042
$R_w(F_o)^a$ for $F_o^2 > 3\sigma(F_o^2)$	0.055

^{a} $R(F_o^2) = \sum|F_o^2 - F_c^2|/\sum F_o^2$; $R_w(F_o^2) = [\sum w(F_o^2 - F_c^2)^2/\sum wF_o^4]^{1/2}$; $R(F_o) = \sum||F_o| - |F_c||/\sum|F_o|$; $R_w(F_o) = [\sum w'(|F_o| - |F_c|)^2/\sum w'F_o^2]^{1/2}$, where $w = 1/\sigma^2(F_o^2)$ and $w' = 4wF_o^2$.

X-ray Diffraction Study. X-ray data from a single crystal of Co(tbp)I were collected on an Enraf-Nonius CAD4 diffractometer at 125 K. An initial search produced a tetragonal cell, Laue symmetry $4/mmm$, with cell constants a = 14.129 (3) Å and c = 6.334 (1) Å, essentially the same as those of Ni(tbp)I.[6] Systematic absences were observed for the reflections hhl and $0kl$ with l odd, consistent with the space groups $P4/mcc$ and $P4cc$. We have previously reported a series of isostructural compounds of the formula M(L)I, where L = pc, tatbp, and tbp, that crystallize in space group $P4/mcc$.[3a,4,5a,6,7] We therefore chose D_{4h}^2 – $P4/mcc$ as the space group for Co(tbp)I and, not surprisingly, the structure refined successfully. Intensity data were collected by the θ–2θ scan technique and were processed by methods standard in this laboratory.[19] No systematic change was observed in the intensities of six standard reflections measured every 3 h of X-ray exposure time. A total of 2351 reflections were observed. After correction for absorption, these were averaged to yield 720 unique data, of which 486 had $F_o^2 > 3\sigma(F_o^2)$. Experimental details are summarized in Table I. Further details are given in Table SI.[20]

The Patterson map calculated for Co(tbp)I was essentially identical to those calculated for the previous M(L)I compounds. We therefore used the atomic positions of Cu(tatbp)I as a starting solution. The initial isotropic least-squares refinement on F yielded values of R and R_w of 0.11 and 0.12, respectively. Introduction of anisotropic thermal parameters reduced these to 0.043 and 0.055, respectively. All hydrogen atoms were located on a difference electron density map and their positions were idealized (C–H = 0.95 Å) and not varied. Each hydrogen atom was assigned a thermal parameter 1 Å^2 greater than the equivalent isotropic thermal parameter of the carbon atom to which it is bonded. The final refinement was carried out on F_o^2 and involved 65 variables and all 720 unique data. This refinement converged to the agreement indices given in Table I. Final positional and equivalent isotropic thermal parameters are given in Table II. Table SII presents anisotropic thermal parameters.[20]

Single-Crystal Reflectance Spectroscopy. Polarized specular reflectance spectra were obtained with the use of an instrument described in detail elsewhere.[21] Spectra were recorded from the (010) face of Co(tbp)I with the electric vector aligned either parallel or perpendicular to the needle (c) axis of the crystal. For each spectrum, 400 data points were collected between 215 and 850 nm. Collection at each data point proceeded until the sample mean had a 99% probability of being within 1% of the population mean. These spectra were averaged once the data were corrected for percent reflectivity relative to an NIST standard mirror. For Kramers–Krönig analysis[22,23] reflectivities beyond our experimental range were obtained from literature values for the infrared[3c,4] region and were approximated for the vacuum ultraviolet region so as to produce baselines approaching zero absorbance in regions known to have no absorbance in related systems in the vapor state.[24] Deconvolution was carried out with an interactive Gaussian and Lorentzian analysis procedure.

(14) (a) Tsutsui, M.; Velpaldi, R. A.; Hoffman, L.; Suzuki, K.; Ferrari, A. *J. Am. Chem. Soc.* **1969**, *91*, 3337–3341. (b) Datta-Gupta, N. *Inorg. Chem.* **1971**, *33*, 4219–4225.
(15) (a) Salehi, A.; Oertling, W. A.; Babcock, G. T.; Chang, C. K. *J. Am. Chem. Soc.* **1986**, *108*, 5630–5631. (b) Oertling, W. A.; Salehi, A.; Chung, Y. C.; Leroi, G. E.; Chang, C. K.; Babcock, G. T. *J. Phys. Chem.* **1987**, *91*, 5887–5898.
(16) Vogler, A.; Kunkely, H. *Angew. Chem., Int. Ed. Engl.* **1978**, *17*, 760.
(17) Barrett, P. A.; Dent, C. E.; Linstead, R. P. *J. Chem. Soc.* **1936**, 1719–1736.
(18) Shriver, D. F.; Dunn, J. B. R. *Appl. Spectrosc.* **1974**, *28*, 319–323.
(19) Corfield, P. W. R.; Doedens, R. J.; Ibers, J. A. *Inorg. Chem.* **1967**, *6*, 197–204.
(20) Supplementary material.
(21) Desjardins, S. R.; Penfield, K. W.; Cohen, S. L.; Musselman, R. L.; Solomon, E. I. *J. Am. Chem. Soc.* **1983**, *105*, 4590–4603.
(22) Anex, B. G. *Mol. Cryst.* **1966**, *1*, 1–36.
(23) Krönig, R. de L. *J. Opt. Soc. Am.* **1926**, *12*, 547–557.
(24) Edwards, L.; Gouterman, M. *J. Mol. Spectrosc.* **1970**, *33*, 292–310.

Table II. Positional and Equivalent Isotropic Thermal Parameters[a] ($Å^2$) for Co(tbp)I

atom	x	y	z	B
I	1/2	1/2	1/4	2.87 (3)
Co	0	0	0	1.04 (4)
N	0.127 32 (34)	0.059 22 (35)	0	1.0 (1)
C(1)	0.148 39 (41)	0.154 47 (41)	0	1.1 (2)
C(2)	0.249 55 (43)	0.170 23 (40)	0	1.0 (1)
C(3)	0.305 30 (48)	0.251 15 (44)	0	1.8 (2)
C(4)	0.402 43 (46)	0.240 39 (47)	0	1.8 (2)
C(5)	0.443 07 (43)	0.150 90 (47)	0	2.1 (2)
C(6)	0.388 98 (43)	0.070 29 (47)	0	1.6 (2)
C(7)	0.290 90 (43)	0.080 12 (41)	0	1.2 (1)
C(8)	0.213 52 (40)	0.014 23 (41)	0	1.2 (2)
C(9)	0.082 90 (43)	0.225 49 (40)	0	1.3 (2)
H(1)C(3)	0.277	0.314	0	2.7
H(1)C(4)	0.444	0.296	0	2.7
H(1)C(5)	0.511	0.145	0	3.1
H(1)C(6)	0.418	0.008	0	2.6
H(1)C(9)	0.107	0.290	0	2.2

[a] $B_{eq} = (8\pi^2/3)\sum_i\sum_j U_{ij} a_i^* a_j^* \mathbf{a}_i \cdot \mathbf{a}_j$.

Charge Transport Measurements. Single-crystal conductivity measurements on Co(tbp)I were performed, as described elsewhere,[25] by means of a low-frequency four-probe ac technique on crystals that typically were 2–3 mm long and 0.02–0.05 mm wide. The magnetoconductance of single crystals was measured over a temperature range 300–3 K and fields up to 5 T through use of a low-frequency four-probe ac method[26] and a Quantum Design SQUID susceptometer.

The technique used for measuring thermopower was similar to that described by Chaikin and Kwak.[27] A slow alternating temperature gradient with a maximum temperature drop of less than 1 K was employed along the needle-shaped crystals. The thermopower, S, was measured against that of pure gold, the contact material being Pd paint. All data were corrected for the thermopower of gold.

Electron Paramagnetic Resonance Measurements. EPR spectra at ca. 9 GHz were obtained on a modified Varian E-4 spectrometer. Spectra were recorded at ambient temperature and 77 K.

Magnetic Susceptibility Measurements. Static magnetic susceptibility measurements were taken from 220 to 1.85 K with a SHE VTS-10 SQUID susceptometer. Sample holders made of high-purity Suprasil quartz were employed. The background was obtained over the full temperature range just prior to measuring the sample. Calibration of the instrument was routinely checked with Au as a standard. Sample sizes varied from 15 to 40 mg.

Results

Preparation and Purification of Zn(tbp) and Co(tbp). Until now, the synthesis of Zn(tbp) has been plagued by the presence of a porphyrin-like impurity regardless of the synthetic route and despite extensive purification.[28] The unidentified impurity has a distinct peak at 460 nm in the UV–vis spectrum, to the red of the peak at 433 nm. Recrystallization of Zn(tbp) from 1-chloronaphthalene virtually eliminates the 460 nm peak (Figure 1A,B). Demetalation of Zn(tbp) and remetalation yield Co(tbp), whose solution spectrum shows characteristic peaks for metallotetrabenzoporphyrins at 404, 426, and 612 nm,[28] but nothing at 460 nm.

Resonance Raman Spectroscopy. The resonance Raman spectrum of polycrystalline Co(tbp)I at room temperature exhibits a sharp fundamental peak at 110 cm^{-1} with an overtone progression of peaks at 216, 320, and 428 cm^{-1}. This pattern is characteristic of linear chains of symmetrical triiodide ions.[29] The absence of any observable peaks having an intensity larger than that of the overtone band at either 167 or 212 cm^{-1} eliminates I_5^- or I_2 as the predominant form of iodine in this material. By analogy with Ni(pc)I,[3a] for which ^{129}I Mössbauer experiments provided no evidence for the presence of I^-, we conclude that the proper formulation of Co(tbp)I is $[Co(tbp)]^{0.33+}[I_3^-]_{0.33}$, with partial oxidation of 1/3 electron per metallomacrocycle.

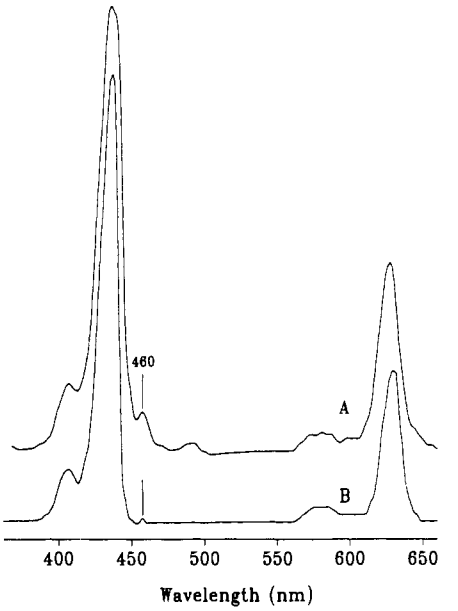

Figure 1. UV–visible spectra of Zn(tbp) in 1-chloronaphthalene (A) before and (B) after recrystallization from 1-chloronaphthalene. Note the decrease in the intensity of the peak at 460 nm, as shown by the lines.

Description of the Structure. The structure of Co(tbp)I is essentially identical to those of H_2(tbp)I, Ni(tbp)I, and other M(L)I molecular conductors.[3a,4,5a,6,7,30] It comprises columns of Co(tbp) cations surrounded by chains of I_3^- anions. These Co(tbp) units have crystallographically imposed $4/m$ symmetry and are thus constrained to be planar. The cations stack metal-over-metal with their molecular planes normal to the c axis and separated by $c/2 = 3.167$ (1) Å. This is to be compared with the separation of $c/2 = 3.123$ (1) Å for Co(pc)I.[4] The two rings in the unit cell of Co(tbp)I are staggered by 40.3 (7)°, similar to the values found in Co(pc)I and the other M(L)I compounds. The anion chains lie within the channels formed by the benzo groups of the Co(tbp) cations and run parallel to the c axis.

A drawing of the Co(tbp) cation with labeling scheme is shown in Figure 2. Table III summarizes the intramolecular bond distances and angles determined for Co(tbp)I at 125 K. The central hole of the Co(tbp) cation is larger than that of Co(pc); the Co–N, Co–C(1), Co–C(8), and Co–C(9) bond distances are 0.066 (6), 0.086 (10), 0.087 (10), and 0.028 (10) Å greater than their Co(pc) counterparts. In addition, the methine bridge angle [C(1)–C(9)–C(8)] is 5.6 (7)° greater than the corresponding azomethine bridge in Co(pc). Apparently, the lone-pair electrons on the methine nitrogen atom have a greater steric effect than does the methine hydrogen atom, and this leads to the contraction of the azomethine bridge angle.[31] Similar comparisons have been made between Ni(tbp)I and Ni(pc)I. All bond distances and angles in the Co(tbp) cation agree with those found for the Ni(tbp) cation in Ni(tbp)I within experimental error.[6]

The iodine atom is on a site of 422 symmetry. Its root-mean-square amplitude of vibration along the chain direction is 3 times that perpendicular to it. This has been observed in all the M(L)I

(25) Phillips, T. E.; Anderson, J. R.; Schramm, C. J.; Hoffman, B. M. *Rev. Sci. Instrum.* **1979**, *50*, 263–265.
(26) Thompson, J. A.; Murata, K.; Miller, D. E.; Stanton, J. L.; Broderick, W. E.; Hoffman, B. M.; Ibers, J. A. Manuscript in preparation.
(27) Chaikin, P. M.; Kwak, J. F. *Rev. Sci. Instrum.* **1975**, *46*, 218–220.
(28) (a) Remy, D. E. *Tetrahedron Lett.* **1983**, *24*, 1451–1454. (b) Edwards, L.; Gouterman, M.; Rose, C. B. *J. Am. Chem. Soc.* **1976**, *98*, 7638–7641. (c) Linstead, R. P.; Weiss, F. T. *J. Chem. Soc.* **1950**, 2975–2987.
(29) (a) Teitelbaum, R. C.; Ruby, S. L.; Marks, T. J. *J. Am. Chem. Soc.* **1978**, *100*, 3215–3217. (b) Teitelbaum, R. C.; Ruby, S. L.; Marks, T. J. *Ibid.* **1980**, *102*, 3322–3328.
(30) Murata, K.; Liou, K. K.; Thompson, J. A.; McGhee, E. M.; Hoffman, B. M.; Ibers, J. A. Manuscript in preparation.
(31) Hoard, J. L. In *Porphyrins and Metalloporphyrins*; Smith, K. M., Ed.; American Elsevier: New York, 1975; pp 321–327.

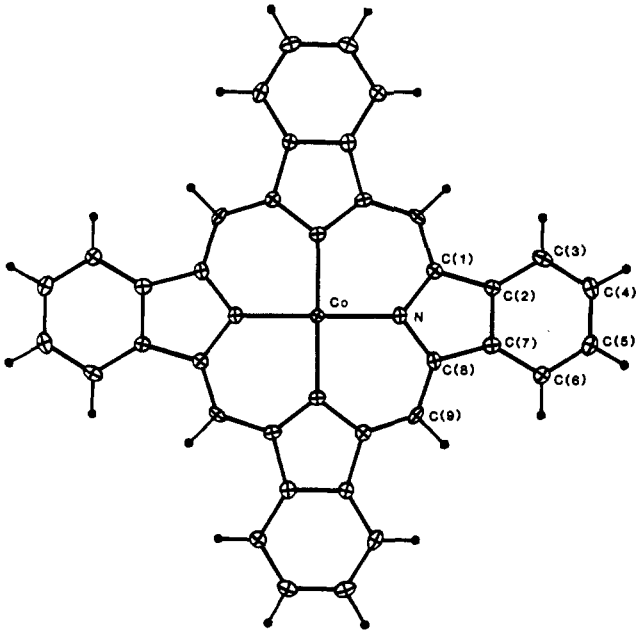

Figure 2. Drawing of the Co(tbp) cation with labeling scheme. Thermal ellipsoids are drawn at the 50% level. Hydrogen atoms have been omitted for clarity.

systems studied to date[3a,4,5a,6,7a,8,30,32] and is a manifestation of ordered chains of I_3^- ions that are disordered with respect to their neighbors. A detailed analysis of the diffuse X-ray scattering arising from this disorder has been made.[3a,32]

Single-Crystal Reflectance Spectroscopy. Because the high extinction coefficients for Co(tbp)I prevent the use of absorbance techniques for electronic spectroscopy, we have used polarized specular reflectance spectroscopy. The energy of metal-to-ligand and ligand-to-metal charge-transfer transitions have been shown to be dependent upon the nature of the central metal.[33,34] From these measurements, we can determine the relative energies of the metal- and ligand-based orbitals near the Fermi level; these in turn have a direct influence upon the site of partial oxidation in this class of materials. Polarized specular reflectance spectra for a single crystal of Co(tbp)I are shown in Figure 3. Corresponding absorbance spectra obtained through Kramers–Krönig analysis of the reflectance data are shown in Figure 4a,b.

(i) Parallel Polarization. The spectrum obtained with the electric vector parallel to the *c* axis is shown in Figure 4a. Since the molecular planes are perpendicular to *c*, this is the "out-of-plane" direction. Gaussian deconvolution gave a better fit to well-resolved peaks than did Lorentzian deconvolution. It was initiated with two transitions associated with the triiodide anions. In M(pc)I compounds[33,34] there are two I_3^- transitions polarized parallel to the needle axis that occur at ca. 20 000 and 30 000 cm^{-1}. These absorptions, which have been assigned to the $^1\Sigma_g \rightarrow {}^1\Sigma_u^*$ transition and a spin–orbit component, respectively, are indicated as bands D and F in Figure 4a.

An additional transition recently assigned occurs at 25 500 cm^{-1} (band E).[34,35a] Although no such band appears in the solution absorption spectra of I_3^-, similar transitions around 24 000 cm^{-1} appear as shoulders in the absorption spectra of crystalline $[N(n\text{-}Bu)_4]I_3$, (benzamide)$_2$·HI_3, and (caffeine)·H_2O·HI_3.[36] Thus, this band is tentatively ascribed to the triiodide chain in the solid-state environment of the M(tbp)I system, as has been done for the M(pc)I system.[34]

By analogy with Co(pc)I, we assign bands A and G to the metallomacrocycle-based out-of-plane $a_{1g}(d_{z^2}) \rightarrow a_{2u}(p_z,\pi^*)$ and $3b_{2u}(\pi) \rightarrow b_{1g}(d_{x^2-y^2})$ transitions, respectively. Significantly, band A at 18 000 cm^{-1}, is *blue*-shifted by 4000 cm^{-1} compared to the corresponding band in the spectrum of Co(pc)I, while band G at 36 000 cm^{-1} is *red*-shifted by 4000 cm^{-1}. As Co(pc)I and Co(tbp)I are isostructural, these spectral differences must arise primarily from differences in the electronic structures of the constituent Co(pc) and Co(tbp) molecules. Indeed, it is possible to rationalize the observed shifts with qualitative ligand-field and molecular-orbital arguments. Because the central cavity of the tbp ring is larger than that of the pc ring, ligand-field arguments predict that the $a_{1g}(d_{z^2})$ and $b_{1g}(d_{x^2-y^2})$ molecular orbitals of Co(tbp) should be slightly lower in energy than the corresponding orbitals of Co(pc). The substitution of less electronegative methylene carbon atoms in the pyrrole-bridging positions is expected to raise the energies of tbp π-MO's having significant contributions from these sites relative to the corresponding MO's of pc. Thus, the $a_{1g}(d_{z^2}) \rightarrow a_{2u}(p_z,\pi^*)$ transition of Co(tbp)I should be at a higher energy than that of Co(pc)I, and the $3b_{2u}(\pi) \rightarrow b_{1g}(d_{x^2-y^2})$ transition should be at a somewhat lower energy. These results confirm the results of Liang et al.[35] that there is a general increase in the energies of the ligand-based π-bands of tbp relative to those of pc; this effect perhaps is responsible for raising the highest occupied π-band in Co(tbp)I above the lowered level of the $a_{1g}(d_{z^2})$ band sufficiently to lead to ligand-based conduction upon partial oxidation (vide infra).

(ii) Perpendicular Polarization. The visible region of the spectrum with **E** perpendicular to *c* (in-plane) in Figure 4b shows a characteristic pair of peaks around 15 000–20 000 cm^{-1}. The lower energy peak, Q, at 16 400 cm^{-1} is equivalent to one at ~15 500 cm^{-1} in the M(pc)I series and generally has been accepted as $a_{1u}(\pi) \rightarrow e_g(\pi^*)$.[24,33-38] A $2a_{1u}(\pi) \rightarrow 7e_g(\pi^*)$ transition is calculated to lie at 15 136 cm^{-1} in Ni(tbp);[35b] as the corresponding peak positions for Co(pc)I and Ni(pc)I are within 100 cm^{-1} of each other, it is reasonable to assign peak Q as $2a_{1u}(\pi) \rightarrow 7e_g(\pi^*)$. The accompanying peak R at 18 300 cm^{-1} is assigned as primarily $5a_{1u}(\pi) \rightarrow 7e_g(\pi^*)$; this transition appears at 20 710 cm^{-1} in a Ni(tbp) calculation,[35b] so it is again reasonable to correlate peaks for M = Ni and Co, by following the example of the M(pc)I series.

The intense peak B at 27 250 cm^{-1} corresponds to the Soret band in solution spectra. Recently, this band has been reassigned in M(pc) compounds as being primarily $6e_g(\pi) \rightarrow 4b_{2u}(\pi^*)$,[34,35] with minor contributions from several much weaker transitions. The assignment of the B band for porphyrins had been based upon a "four-orbital model"[24,39] in which accidentally degenerate $a_{1u} \rightarrow e_g$ and $a_{2u} \rightarrow e_g$ transitions undergo configuration interaction (CI) to produce two peaks: Q at ~15 000 cm^{-1} and B at ~30 000 cm^{-1}. An equivalent approach for phthalocyanines sets the a_{1u} and a_{2u} orbitals at energies ~15 000 cm^{-1} apart, thus eliminating CI, and attributes the Soret band solely to an $a_{2u}(\pi) \rightarrow e_g(\pi^*)$ transition. Our determination that the Soret band of M(pc) compounds is not an $a_{2u} \rightarrow e_g$ transition calls into question the application of the four-orbital model to Co(tbp). Calculations on Ni(tbp) predict several transitions around 27 000 cm^{-1}, the strongest being $6e_g(\pi) \rightarrow 4b_{2u}(\pi^*)$.[35b] Others include $2b_{1u} \rightarrow 7e_g$ and $4a_{2u} \rightarrow 7e_g$. The $6e_g(\pi) \rightarrow 4b_{2u}(\pi^*)$ transition also was found to be the major contributor to the Soret band in the M(pc) compounds.[35a] We thus tentatively assign band B as being

(32) Stanton, J. L. Ph.D. Dissertation, Northwestern University, Evanston, IL, 1985.
(33) Heagy, M. D.; Rende, D. E.; Shaffer, G. W.; Wolfe, B. W.; Liou, K.; Hoffman, B. M.; Musselman, R. L. *Inorg. Chem.* **1989**, *28*, 283–286.
(34) Rende, D. E.; Heagy, M. D.; Heuer, W. B.; Liou, K.; Thompson, J. A.; Hoffman, B. M.; Musselman, R. L. *Inorg. Chem.* **1992**, *31*, 352–358.
(35) (a) Liang, X.; Flores, S.; Ellis, D. E.; Hoffman, B. M.; Musselman, R. L. *J. Chem. Phys.* **1991**, *95*, 403–417. (b) Liang, X.; Flores, S.; Ellis, D. E. Unpublished results.
(36) Mizuno, M.; Tanaka, J.; Harada, I. *J. Phys. Chem.* **1981**, *85*, 1789–1794.
(37) Chen, I. *J. Mol. Spectrosc.* **1967**, *23*, 131–143.
(38) (a) Schaffer, A. M.; Gouterman, M.; Davidson, E. R. *Theor. Chim. Acta* **1973**, *30*, 9–30. (b) Schaffer, A. M.; Gouterman, M.; Davison, E. R. *Theor. Chim. Acta* **1972**, *25*, 62–82.
(39) Basu, S. *Ind. J. Phys.* **1955**, *28*, 511–521.

Table III. Bond Distances (Å) and Angles (deg) for Co(tbp)I

bond	distance[a]	av[b]	bond	distance	av
Co–N	1.984 (5)		C(2)–C(3)	1.388 (9)	
			C(6)–C(7)	1.393 (8)	1.391 (9)
N–C(1)	1.378 (7)				
N–C(8)	1.374 (7)	1.376 (7)	C(3)–C(4)	1.381 (9)	
			C(5)–C(6)	1.372 (9)	1.377 (9)
C(1)–C(2)	1.447 (8)				
C(7)–C(8)	1.436 (8)	1.442 (8)	C(4)–C(5)	1.389 (9)	
C(2)–C(7)	1.401 (8)		C(9)–C(1)	1.365 (8)	
			C(9)–C(8)	1.383 (8)	1.374 (8)
Co–Co′	3.167 (1)				

type	angle	av	type	angle	av
N–Co–N′	180		C(1)–C(9)–C(8)	125.6 (6)	
Co–N–C(1)	127.4 (4)		N–C(1)–C(9)	124.9 (6)	
Co–N–C(8)	127.5 (4)	127.5 (4)	N–C(8)–C(9)	124.6 (5)	124.7 (6)
C(1)–N–C(8)	105.1 (5)		N–C(1)–C(2)	111.3 (5)	
			N–C(8)–C(7)	112.0 (5)	111.7 (5)
C(9)–C(1)–C(2)	123.8 (5)		C(3)–C(2)–C(7)	120.8 (5)	
C(9)–C(8)–C(7)	123.4 (5)	123.6 (5)	C(6)–C(7)–C(2)	120.4 (6)	120.6 (6)
C(1)–C(2)–C(3)	133.4 (6)		C(2)–C(3)–C(4)	118.2 (6)	
C(6)–C(7)–C(8)	133.9 (6)	133.7 (6)	C(5)–C(6)–C(7)	118.1 (6)	118.2 (6)
C(1)–C(2)–C(7)	105.8 (5)		C(3)–C(4)–C(5)	120.7 (6)	
C(2)–C(7)–C(8)	105.8 (5)	105.8 (5)	C(4)–C(5)–C(6)	121.7 (6)	121.2 (7)

[a] Angle between two Co(tbp) units in the cell, 40.3 (7)°. [b] Average values are weighted. The error is taken to be the larger of the unweighted estimated standard deviation of a single observation and that estimated from the inverse matrix.

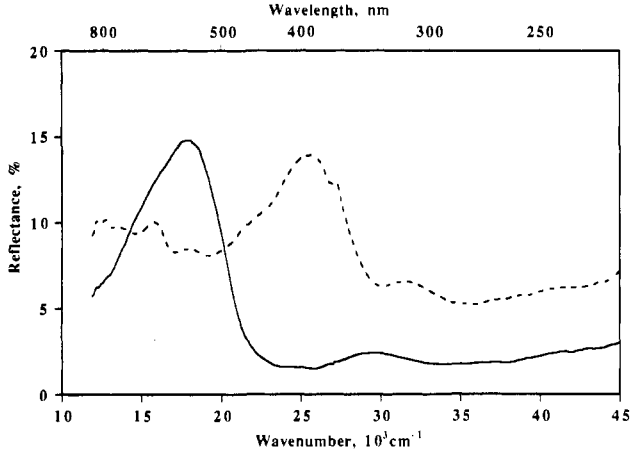

Figure 3. Polarized specular reflectance of Co(tbp)I: (—) parallel to needle (out of plane); (- - -) perpendicular to needle (in plane).

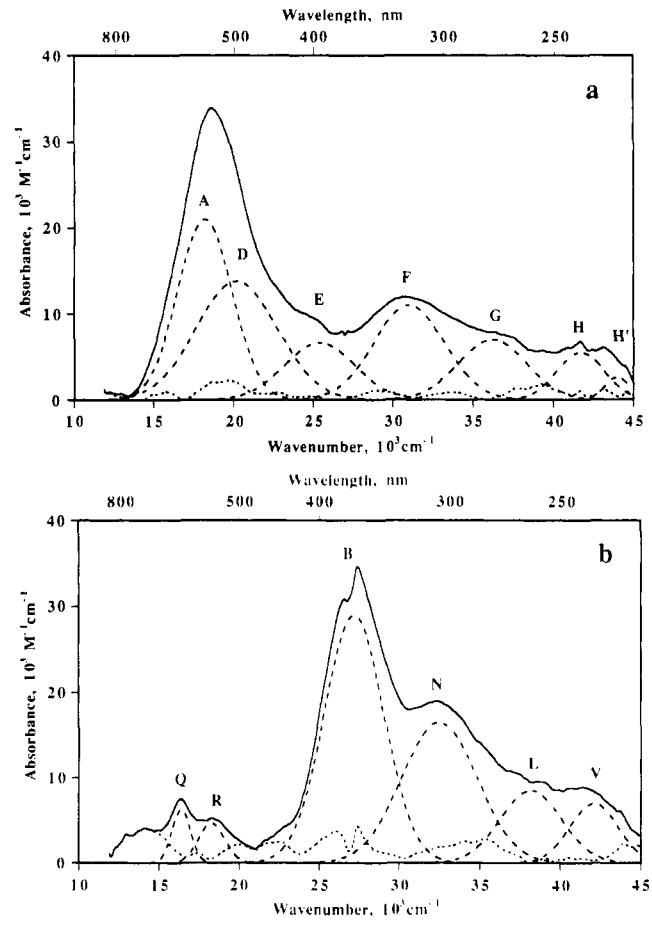

Figure 4. (a) Out-of-plane absorbance from specular reflectance of Co(tbp)I: (—) experimental; (- - -) Gaussian deconvolution. (b) In-plane absorbance from specular reflectance of Co(tbp)I: (—) experiemntal; (- - -) Gaussian deconvolution.

primarily $6e_g(\pi) \rightarrow 4b_{2u}(\pi^*)$ with contributions from $2b_{1u}(\pi) \rightarrow 7e_g(\pi^*)$ and $4a_{2u}(\pi) \rightarrow 7e_g(\pi^*)$. The structure on peak B we believe to be instrument noise because the corresponding peaks in M(pc)I compounds[33,34] and preliminary spectra on Ni(tbp)I, H_2(tbp)I, and Cu(tbp)I show no structure.[40] The peaks labeled N, L, and V fall in the region in which at least five moderately intense ($0.14 \leq f \leq 0.51$) transitions are predicted for Ni(tbp): $6e_g \rightarrow 3b_{1u}$, $6e_g \rightarrow 6a_{2u}$, $5e_g \rightarrow 3b_{1u}$, $2a_{1u} \rightarrow 9e_g$, and $2b_{1u} \rightarrow 8e_g$.[35b] Presumably, these five contribute to much of the intensity in this region.

Conductivity. The room-temperature conductivity (σ_{RT}) of Co(tbp)I is comparable to that of other ligand-centered π-conductors (500 Ω^{-1} cm^{-1})[3a,5a,6] and is 10 times that of Co(pc)I.[4] As the temperature is lowered, the conductivity initially increases in a metallic fashion ($d\sigma/dT < 0$, for $300 > T > 170$ K) as does that of the M(L)I (M = Ni, Cu, "H_2") ring-oxidized conductors (see Figure 5). In contrast, for the isostructural analogue Co(pc)I, which is a metal-spine semiconductor, $\sigma(T)$ decreases in a roughly linear fashion from $\sigma_{RT} \approx 50$ Ω^{-1} cm^{-1} as the temperature is lowered.[4] Thus, the conductivity data place Co(tbp)I with the ring-centered conductors, rather than with Co(pc)I. The occurrence of a conductivity maximum at a relatively high temperature ($T_{max} \sim 170$ K)[41] we attribute to scattering of the conduction electrons by the interaction with the local moments of the Co^{2+} spins. This type of strong spin–spin interaction has been seen in Cu(pc)I, as well as in Cu_xNi_{1-x}(pc)I alloys.[5,10]

(40) Rende, D. E.; Heagy, M. D.; Musselman, R. L. Manuscript in preparation.

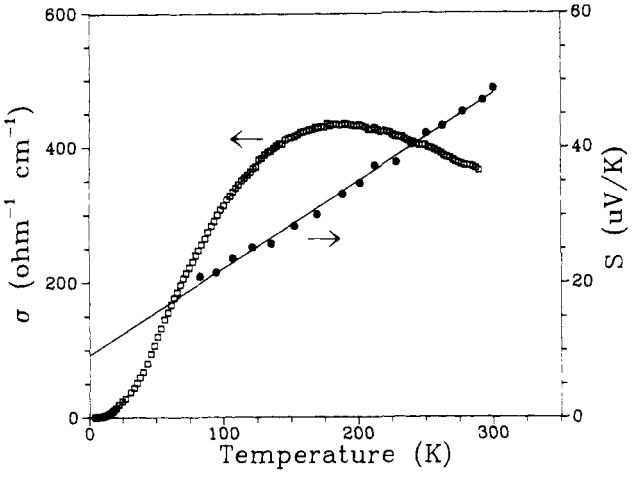

Figure 5. Temperature dependence of the conductivity along the stacking axis for a single crystal of Co(tbp)I (□) and the thermoelectric power (●) of Co(tbp)I. The solid line is present only to guide the eye.

To investigate further the charge transport properties of Co(tbp)I, we attempted to measure the transverse magnetoconductance. If an external magnetic field could partially orient the local moments, this would diminish the scattering of the conduction electrons and increase the conductivity. However, the application of a 5-T field did not result in a detectable change in the conductivity ($\Delta\sigma/\sigma < 0.02$) at any temperature between 3 and 300 K. We attribute the lack of magnetoconductance to coupling between the local moments of Co^{2+} that is much greater than the electron Zeeman energy at 5 T (~ 5 cm^{-1}).

Thermoelectric Power. Thermoelectric power measurements confirm that Co(tbp)I is a ring-oxidized molecular metal. The temperature dependence of the Seebeck coefficient (S) in the range 80–300 K is shown in Figure 5. The room-temperature value is about +50 V/K and decreases linearly to +20 V/K at 80 K. This behavior is similar to that of other ring-oxidized M(L)I conductors, such as Ni(pc)I[3c] and Cu(pc)I,[5a] both of which exhibit a positive thermopower and a linear temperature dependence. Such a well-behaved and positive thermopower in these cases indicates that the charge carriers are holes in the more than half-filled pπ-ligand orbital band: the one-third oxidation per doubly filled macrocycle HOMO corresponds to a π-band five-sixths-filled with electrons, which is equivalent to one-sixth hole filling. In contrast, if oxidation were to occur at the metal, the d_{z^2} band would be half-filled before oxidation. After oxidation of $^1/_3$ electron per metal, the d_{z^2} band would be one-third filled with electrons. The conductivity of a less than half-filled band is associated with the electrons, and the thermopower would be negative. This behavior is in fact seen for Co(pc)I.

In the tight-binding model, the thermopower for a one-dimensional metal varies linearly with temperature, as seen in Figure 5, and may be written[42] (neglecting correlation effects) as

$$S = -\frac{2\pi^2}{3}\left(\frac{k_B}{e}\right)\frac{k_B T}{W}\left\{\frac{\cos(\pi\rho/2)}{\sin^2(\pi\rho/2)} + \frac{W}{2}\frac{\tau'(\epsilon)}{\tau(\epsilon)}\bigg|_{E_F}\right\} \quad (1)$$

where ρ is the number of conduction electrons per molecule, W is the bandwidth, and $\tau(\epsilon)$ is the carrier scattering time (and energy derivative) at the Fermi level, E_F. For simple phonon-scattering, the two terms in the bracket are equal. If we take this to hold, then eq 1 gives $W = 1.3$ eV, similar to the value for M(pc)I, M = Ni, Cu.[3c,5a] However, this model requires that $S(T)$ extrapolate to zero at 0 K. Because this behavior clearly is not followed (Figure 5) and because the dominating scattering mechanism is unknown, the derived value of W should be regarded with caution.

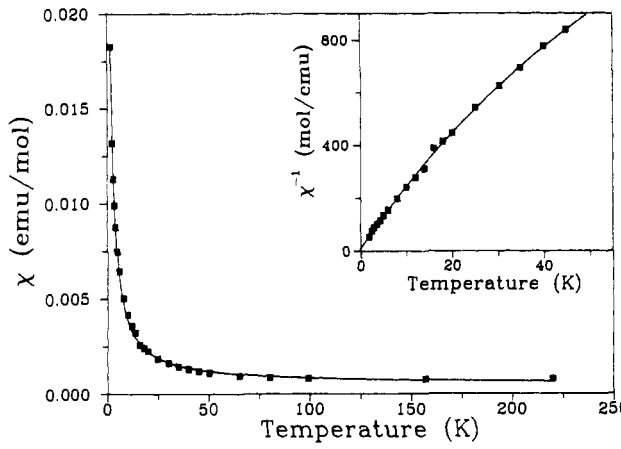

Figure 6. Bulk magnetic susceptibility χ (emu/mol) vs T. Inset: plot of χ^{-1} vs T over the range $2 < T < 50$ K.

Magnetic Measurements. The static magnetic susceptibility of Co(tbp)I, measured at 220 K and corrected for the diamagnetism of the ring and the metal, is 7.8×10^{-4} emu/mol. The temperature dependence of the susceptibility has been measured between 1.85 and 220 K (Figure 6). In the range from 220 to 50 K, the susceptibility is nearly temperature independent, $\chi = 8 \times 10^{-4}$ emu/mol, similar to the behavior of ring-oxidized M(L)I compounds where the divalent metal is diamagnetic, for example Ni(L)I.[3,6] As the temperature is lowered below $T \sim 50$ K, the susceptibility data show an additional Curie–Weiss contribution with $C = 0.039$ (emu K)/mol and $\Theta = 0.39$ K.[43]

Because oxidation of the ring leaves one $S = {}^1/_2$ Co^{2+} ion per site, one might expect the high-temperature magnetic susceptibility of Co(tbp)I to be similar to that for the ring-oxidized materials Cu(L)I, L = pc, tatbp, which is described by a temperature-independent Pauli susceptibility associated with the organic charge carriers and a temperature-dependent Curie–Weiss contribution with a measured Curie constant of $C = 0.402$ (emu K)/mol, as expected for a linear chain of Cu^{2+} ($S = {}^1/_2$) spins.[5,7] However, the magnetic susceptibility of Co(tbp)I is very different. The value of C for Co(tbp)I of 0.039 (emu K)/mol is approximately one-tenth the expected value for a chain of Co^{2+} ($S = {}^1/_2$) ions. We interpret the reduced susceptibility for Co(tbp)I as resulting from strong antiferromagnetic coupling among the spins of the cobalt ions, as is also suggested by the absence of a detectable magnetoconductance. This coupling likely reflects a combination of direct overlap between neighboring spins in the half-occupied Co (d_{z^2}) orbitals, along with long-range, indirect, carrier-mediated coupling. The Curie tail could result from crystal defects or impurities that leave uncoupled Co^{2+} sites or from the defects and impurities themselves.[44,45] Most likely, the coupling in Co(tbp)I is stronger than that in the Cu(L)I compounds (L = pc, tatbp) because the unpaired electron on Cu^{2+} is in the in-plane $d_{x^2-y^2}$ orbital whereas the unpaired electron on Co^{2+} is in the out-of-plane d_{z^2} orbital. There can be very little overlap of adjacent $d_{x^2-y^2}$ orbitals, separated by ~ 3.2 Å.

The EPR spectrum of Co(tbp)I at ambient temperature shows a single weak signal at $g = 2.00$, with a line width $\Gamma \approx 4$ G, as

(41) (a) For Co(tbp)I, the conductivity normalized to the room-temperature value can be fit with the expression[41b] $\sigma_n(T) = AT^{-\alpha}\exp(-\Delta_\sigma/(kT))$ for $300 > T > 50$ K, yielding $\alpha = 0.92$ and $\Delta_\sigma/k = 169$ K. However, the model that led to this equation and the corresponding interpretation is not relevant here. (b) Epstein, A. J.; Conwell, E. M.; Sandman, D. J.; Miller, J. S. *Solid State Commun.* **1977**, *23*, 355–358.

(42) Chaikin, P. M.; Greene, R. L.; Etemad, S.; Engler, E. *Phys. Rev. B* **1976**, *13*, 1627–1632.

(43) Magnetic susceptibility data for $1.9 < T < 50$ K were fit to the Curie–Weiss law plus a Pauli term, $\chi = C/(T - \Theta) + \chi_P$.

(44) Diel, B. N.; Inabe, T.; Lyding, J. W.; Schoch, K. F.; Kannewurf, C. R.; Marks, T. J. *J. Am. Chem. Soc.* **1983**, *105*, 1551–1567.

(45) Delhaus, P.; Coulon, C.; Flandrois, S.; Hilti, B.; Mayer, C. W.; Rihs, G.; Rivory, J. J. *J. Chem. Phys.* **1980**, *73*, 1452–1463.

seen in Co(pc)I.[4] Spectra recorded at 77 K do not show any new features. Since the intensity of the EPR signal from Co(tbp)I is approximately $^1/_{1000}$th of that from Ni(pc)I, where it is assigned to the carrier spins, we assign the signal to impurities and conclude that both the intrinsic charge carriers and Co^{2+} spins are EPR silent.

Discussion

We have shown previously that changing the central metal from Ni or Cu to Co in the M(pc)I system causes a dramatic change in charge-transport properties. The charge carriers in Ni(pc)I and Cu(pc)I are holes that propagate through the highest-occupied delocalized orbitals of pc.[3a,5] However, the charge carriers for Co(pc)I are electrons, and charge transport is along the Co metal spine.[4] The present investigation examines the influence of the isostructural change from the pc to the tbp macrocyclic ligand. The conductivity and thermoelectric power measurements show that Co(tbp)I is a ligand-centered conductor, unlike Co(pc)I. The change from partial metal oxidation in Co(pc)I (formally $Co^{2.33+}$) to ring oxidation in Co(tbp)I (formally Co^{2+}) undoubtedly occurs because the porphyrin ring is easier to oxidize than is the phthalocyanine ring. Comparison of the single-crystal reflectance spectroscopy for Co(pc)I and Co(tbp)I shows that the $p\pi$-orbitals for Co(tbp)I are somewhat higher in energy than are the corresponding orbitals for Co(pc)I. The energy difference is enough to elevate the $p\pi$-HOMO above the metal-based d_{z^2} orbital in Co(tbp)I and to cause partial oxidation to occur at the ring, not the metal ion. Calculations of energies for several M(pc)I compounds and for Ni(tbp)I confirm that $p\pi$-bands are lower in energy for Ni(tbp)I relative to Ni(pc)I.[35] Other M(tbp)I crystals currently are being studied spectroscopically, and it is expected that systematic correlations in the M(tbp)I series will be found.

Partial oxidation at the macrocycle ring to form an M(L)I conductor leaves 1 electron in the d_{z^2} orbital of the metal ion for M = Co and 1 electron per $d_{x^2-y^2}$ for M = Cu. In both cases, as well as in Cu_xNi_{1-x}(pc)I alloys, the spins on the metal ion spine are coupled by a combination of direct interaction between adjacent spins and indirect carrier-mediated long-range interactions. However, the data presented here show that Co–Co couplings are far stronger than are Cu–Cu couplings. Clearly, direct M–M interactions should be stronger for the out-of-plane d_{z^2} orbitals of Co^{2+} than for the in-plane $d_{x^2-y^2}$ orbitals of Cu^{2+}. This by itself may explain the fact that the Cu^{2+} ions show nearly their full Curie contribution,[5,7] whereas the Co–Co couplings are sufficiently strong to render the Co^{2+} ions essentially nonmagnetic. Studies on M_xNi_{1-x}(tbp)I alloys, where M = Co and Cu, would be required to determine whether the long-range couplings are greater for M = Co as well. Here, the interaction arises from $d-\pi$ coupling, and its relative strength in the two cases is difficult to predict. Intramolecular $d-\pi$ coupling is predicted by Liang et al. to be greater for M = Cu.[35a] However, intermolecular coupling between d and π bands for $k \neq 0$ should be greater for M = Co.[46]

The strong coupling among the Co^{2+} spins of Co(tbp)I explains the absence of magnetoconductance, the suppressed susceptibility, and the lack of an EPR signal. We have nonetheless proposed that scattering of the itinerant carriers by the local moments accounts for the minimal increase in conductivity from 300 to 170 K and for the relatively high temperature of the conductivity maximum (T_{max} = 170 K) compared to other ring-oxidized, metallic conductors. For this to be consistent with the absence of magnetoconductance implies that the carriers are scattered by coupling to modes that are not thermally excited.

Acknowledgment. This work was supported by the Solid State Chemistry Program of the National Science Foundation through Grant No. DMR-9144513 (B.M.H.), the Northwestern University Materials Research Center, Grant No. DMR-8821571, the donors of the Petroleum Research Fund, administered by the American Chemical Society (R.L.M.), the National Science Foundation Inorganic, Bioinorganic, and Organometallic Chemistry Program, Grant No. CHE-8911215 (R.L.M.), the Camille and Henry Dreyfus Foundation (New Grant Program in Chemistry for Liberal Arts Colleges to R.L.M.) including a fellowship to W.B.H., and Franklin and Marshall College (Hackman Fellowship to M.D.H.).

Supplementary Material Available: Table SI, giving additional crystallographic details, and Table SII, listing anisotropic thermal parameters (2 pages). Ordering information is given on any current masthead page.

(46) Mott, N. F.; Jones, H. *The Theory of the Properties of Metals and Alloys*; Dover Publications, Inc.: New York, 1958; pp 56–86.